PHYSICAL REVIEW B VOLUME 2, NUMBER 8 15 OCTOBER 1970

Theory of Semiconductor Response to Charged Particles

Werner Brandt and Julian Reinheimer*
Department of Physics, New York University, New York, New York 10003
(Received 4 March 1970)

The wave-number- and frequency-dependent dielectric function of a semiconductor is derived and calculated in terms of a model consisting of an electron gas with an energy gap. From it are deduced, as a function of the gap width, (*i*) the screening of a point defect, (*ii*) the annihilation rate of positrons, and (*iii*) the stopping power for swift charged particles. A partition rule holds between the contributions of single-particle excitations L_s and collective resonance excitations L_r to the stopping number $L = L_s + L_r$ in the sense that $L_s = C + L_r$; the constant C grows with the gap width.

I. INTRODUCTION

In the past the response of condensed matter to the disturbance set up by a charged particle has been investigated extensively in terms of the many-body theory of an extended degenerate electron gas. Among the problems that have been studied are the screening of point defects,[1,2] positron annihilation,[3,4] and the stopping power of matter for heavy charged particles.[5] The method has been applied to atomic systems.[6,7] Recently beginnings have been made to extend the theory to models for semiconductors and insulators. Penn[8] derived the static wave-number-dependent response function for a semiconductor model proposed by Callaway.[9] It consists of an electron gas with an energy gap E_g. Others[10,11] investigated the frequency dependence of the response in the long-wavelength limit.

In an extended study of this model semiconductor, we have derived the full wave-number- and frequency-dependent longitudinal response function in the random-phase approximation and its parametric dependence on E_g. From it, semiconductor properties are calculated and their sensitivity to changes in the energy gap studied. Although the results apply strictly only to the high-density limit, we expect that the emerging trends reflect realistically the effects of the energy gap on the properties of different semiconductors. For a given semiconductor, the degree of internal consistency of this approach can be tested experimentally because all properties so calculated are interrelated through the parameter E_g. This should provide guidance for refining the theory and for expanding the scope of experimental investigations.

In Sec. II we summarize the derivation of the response function and apply it, in Sec. III, to the static screening of charged particles in the model semiconductor. In Sec. IV, the stopping power for swift charged particles is calculated. The principal result is an important partition rule of stopping powers in a solid with an energy gap.

II. RESPONSE FUNCTION

We base our considerations on a model semiconductor consisting of a uniform electron gas of density n with a single energy gap characterized by a gap width E_g. In this model, the valence band is filled, and the formation of standing waves at the Brillouin boundaries and umklapp processes are taken into account. The distribution of the model density of states is constructed such that the states removed from the gap are piled up on either side of the gap. The Fermi surface is placed halfway in the forbidden gap so that the excitations of the system amount to particle-hole excitations across the gap. In real solids the band structure is complicated, and the gap widths and the electron density are not independent parameters. Therefore, when comparing the theory with experiments, E_g is taken to be an adjustable parameter characteristic of a given semiconductor. As $E_g \to 0$, the umklapp terms vanish and we retrieve the response of the uniform electron gas.

The response of the system to an external electric field of wave number $\vec{q}$ and frequency ω is described by the dielectric function[12]

$$\kappa(\vec{q}, \omega, E_g) = 1 - (4\pi/q^2)\, h(\vec{q}, \omega, E_g). \tag{1}$$

The response function h can be written in the extended zone scheme,

$$h(\vec{q}, \omega, E_g) = (2\pi)^{-3} \sum_{\vec{K}} \int_{k<k_F} d^3k \left| M(\vec{k}, \vec{k}+\vec{q}+\vec{K}; E_g) \right|^2 \times \{[\omega - E(\vec{k}+\vec{q}+\vec{K}) + E(\vec{k}) + i\eta]^{-1} - [\omega + E(\vec{k}+\vec{q}+\vec{K}) - E(\vec{k}) + i\eta]^{-1}\}. \tag{2}$$

The sum over the reciprocal lattice vectors $\vec{K}$ includes the summation over the valence and conduction bands. The Fermi momentum k_F is related to the electron density n by $k_F = (3\pi^2 n)^{1/3}$, the Fermi velocity $v_F = k_F$ (a.u.), and the Fermi energy $E_F = \frac{1}{2} k_F^2$. The matrix element M connects transitions

between the state of energy $E(\vec{k})$ in the valence band and the state of energy $E(\vec{k}+\vec{q}+\vec{K})$ in the conduction band, subject to the restrictions imposed by the energy gap E_g. Equation (2) is derived in the zero limit of the damping constant η.

The calculations incorporate an approximate formulation for the matrix element, proposed by Penn.[8] It interpolates between the correct asymptotic limits for large and small values of the parameter $z = q/2k_F$. The approximations impose limits on the two parameters of the semiconductor model, viz., the electron density and the energy-gap width. We require the electron density to be high enough for the parameter

$$\chi^2 = e^2/\pi\hbar v_F = r_s/6.02 \tag{3}$$

to be small compared to 1; χ^2 is proportional to the ratio of the Coulomb interaction between the electrons $\sim r_s^{-1}$, and the Fermi energy $\sim r_s^{-2}$; in the usual notation $r_s = (3/4\pi n)^{1/3}$. The other model parameter $\epsilon_g = E_g/E_F$ must be small compared to 1. The quantity $\gamma \equiv \frac{1}{4}\epsilon_g = \frac{1}{4}E_g/E_F$ occurs naturally as an expansion parameter. Another parameter of smallness, viz., $(E_g/\omega_p) = (\sqrt{3})(\gamma/\chi)$, appears in the theory; $\omega_p = (4\pi n)^{1/2}$ is the plasma frequency. As shown in Fig. 1, it imposes less stringent limitations on E_g than $\epsilon_g < 1$ in the χ^2 range appropriate for the valence electrons in solids.

Fry[13] calculated the matrix element for insulators by representing the electrons in the conduction band through single orthogonalized plane waves, and the electrons in the valence band through tight-binding wave functions. The resulting q dependence of the static dielectric function for a number of insulators is in close agreement with Penn's interpolation formula. Therefore at least in the static limit, this calculation illustrates that the results are not affected sensitively by the approximation made for $E(\vec{k})$ and for the matrix elements.

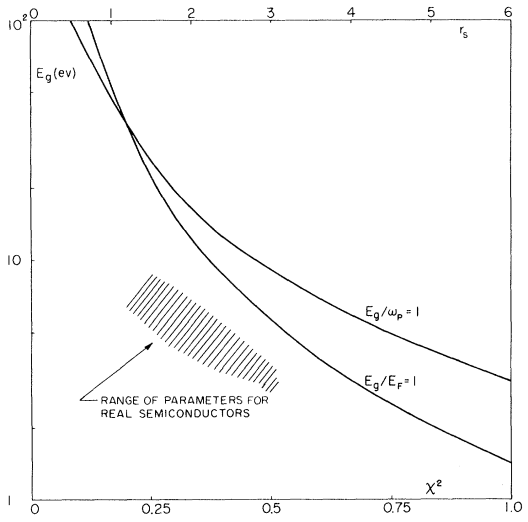

FIG. 1. Validity range of the approximations is bounded by the solid curves.

In calculating $h(\vec{q}, \omega, E_g)$, for a given χ^2, one has to sum over the contributions from the normal and umklapp excitation processes. The general features are conveniently discussed by writing Eq. (2) as a parametric function of the gap parameter in the form

$$\kappa(z, u, E_g) = 1 + g(z, E_g)[f_1(z, u, E_g) + if_2(z, u, E_g)], \tag{4}$$

where

$$g(z, E_g) = \chi^2/(3\gamma^2 + z^2) \tag{5}$$

and

$$z = q/2k_F, \tag{6}$$

$$u = \omega/qv_F \tag{7}$$

are reduced wave vector and frequency variables, respectively. The functions f_1 and f_2 are algebraically complicated. Their display here would be cumbersome but not instructive. They are reported and displayed graphically over ranges of the variables u and z elsewhere; a computer program for their evaluation is available.[14] The dielectric function obeys the sum rule for the oscillator strength distributions $g = (2/\pi)(\omega/\omega_p^2)\mathrm{Im}\kappa^{-1}$,

$$\int_0^\infty d\omega\, g(\vec{q}, \omega, E_g) = 1 \ . \tag{8}$$

The error in the sum rule of the calculations underlying this paper is $\ll \gamma/(1+z^2)$.

In the limit $E_g \to 0$ we make contact with the electron-gas model and obtain Lindhard's dielectric function.[15] In the short-wavelength limit $q \to \infty$, Eq. (4) becomes equal to the dielectric function of the electron gas for any E_g. In the long-wavelength limit $q \to 0$,

$$\kappa(0, \omega, E_g) = 1 - \omega_p^2/[(\omega + i\eta)^2 - E_g^2]. \tag{9}$$

This is the dielectric function describing a simple excitation across a gap of width E_g, corresponding to a vertical transition in the reduced zone scheme. One may use Eq. (9) at $\omega = 0$ to make contact with real materials by adjusting E_g such that $\kappa(0, 0, E_g)$ becomes equal to the static dielectric constant. Table I lists some typical values. For the study of the dynamic response of electrons bound in intermediate shells of atoms or molecules it is often a suitable approximation to retain only the $\vec{K} = 0$ term and to set $E_g \simeq \omega_p$ or $\epsilon_g \simeq r_s^{1/2}$.[16-19]

We have studied in detail the E_g dependence of $\kappa(\vec{q}, 0, E_g)$. Figure 2 illustrates some of the results for the value of $\chi^2 = 0.33$ typical of real semiconductors. The limit $\omega \to 0$ of Eq. (9) determines

TABLE I. Typical semiconductor parameters.

Substance	$\kappa(0,0,E_g)$	χ^2	r_s	ω_p(eV)	ϵ_g	E_g(eV)
Ge	16	0.34	2.04	16	0.35	4.2
Si	12	0.33	1.98	17	0.38	4.8
C(graphite)	8.0	0.35	2.11	15	0.36	4.0
C(diamond)	5.7	0.24	1.44	28	0.54	13.6
Anthracene	3.6	0.40	2.41	12	0.90	5.5
LiH	3.6	0.33	1.98	17	0.82	4.2
AgCl	4.2	0.35	2.11	15	0.79	8.5

the intercept of the curves with the ordinate. When $E_g > 0$, normal and umklapp processes combine to give $\kappa(\vec{q}, 0, E_g)$ a weak maximum [and $\kappa^{-1}(\vec{q}, 0, E_g)$ a minimum] at

$$z_m = q_m/2k_F = (\sqrt{3})\gamma_m\gamma \tag{10}$$

of relative magnitude $(1+\gamma_m^2)$. The value of γ_m depends sensitively on the matrix element just where the interpolation formula is least certain. Our calculations indicate that $\gamma_m \lesssim \gamma$. Other investigators find similar results.[8,13,20,21]

At finite frequencies $\kappa(0, \omega, E_g)$ has a singularity at $\omega = E_g$, or $uz = \gamma$. In coming from low frequencies $\omega < E_g$, or $z < \gamma/u$, the umklapp processes at first dominate the behavior of the system. Figure 3 illustrates this point by showing the ratio f_1(umklapp)/f_1(normal) as a function of z. As the frequency increases, the normal processes begin to dominate and go through a maximum. Normal processes dominate for $\omega > E_g$ or $z > \gamma/u$. The absorptive part f_2 is zero when $\omega < E_g$, rises sharply at $\omega = E_g$ and vanishes as $\sim \omega^{-2}$ in the high-frequency limit. Collective resonances occur when $\kappa(\vec{q}, \omega, E_g) = 0$, as discussed in Sec. IV.

The trends of our results can be summarized concisely by the interpolation formula

$$\kappa(\vec{q}, \omega, E_g) = 1 - \frac{\omega_p^2}{(\omega + i\eta)^2 - E_g^2 + 2\gamma_m E_g s q - s^2 q^2 - \frac{1}{4}q^4} \,. \tag{11}$$

Equation (11) replaces $\kappa_2(\vec{q}, \omega, E_g)$ of the full dielectric function by a δ function. The term containing γ_m is uncertain and in any case small. The last term, $\frac{1}{4}q^4$, accounts for the strong q dependence introduced by quantum-mechanical effects. Since this term is independent of n or χ^2, the function κ in the high-q limit defies scaling in terms of the electron density in a unified way. At moderate q, Eq. (11) reduces to the dielectric function in the semiclassical approximation

$$\kappa(\vec{q}, \omega, E_g) = 1 - \omega_p^2/[(\omega + i\eta)^2 - E_g^2 - s^2q^2]. \tag{12}$$

The constant s is given by $s^2 = (\frac{3}{5})v_F^2$ when $\omega > qv_F$, and by $s^2 = (\frac{1}{3})v_F^2$ when $\omega < qv_F$.[22]

The dispersion relation for longitudinal collective excitations, defined by $\kappa = 0$,

$$\omega^2 = \omega_p^2 + E_g^2 + s^2q^2 + \tfrac{1}{4}q^4 \quad , \tag{13}$$

is at the root of a wide range of phenomena connected with the excitation of electrons bound in dense media.[7,17]

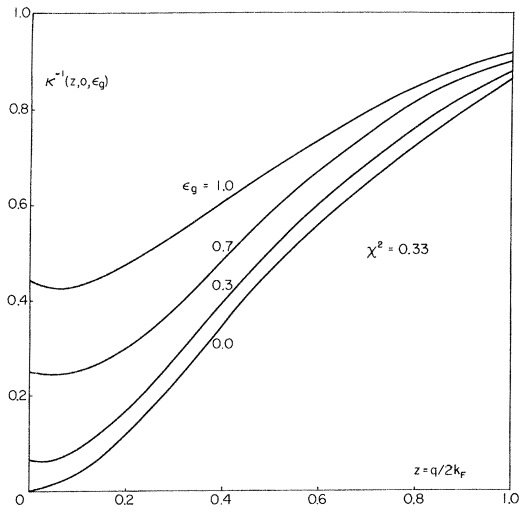

FIG. 2 Reciprocal static dielectric function $\kappa^{-1}(\vec{q}, 0, E_g)$ at $r_s = 2$ as a function of E_g.

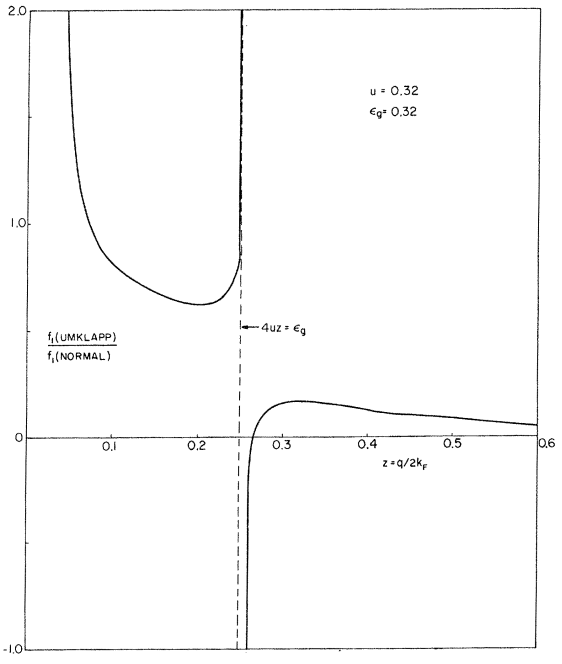

FIG. 3. Ratio of contributions of umklapp and normal processes to the real part of the response function at frequencies corresponding to $u = 0.32$.

III. SCREENING OF POINT CHARGE

In this section we illustrate some of the salient features of the screening of a point charge $Z_1 e$ fixed in the semiconductor discussed elsewhere.[23] The potential V is screened as given by the function

$$\frac{rV(r, E_g)}{Z_1 e} = \frac{2}{\pi}\int_0^\infty dx \frac{\sin x}{x} \kappa^{-1}\left(\frac{\pi\chi^2 x}{2r}, 0, E_g\right). \quad (14)$$

In the limit of large r, and in any case for large E_g, the screening function tends to the usual screened Coulomb potential $(rV/Z_1 e) = \kappa^{-1}(0, 0, E_g)$. When E_g is small Eq. (14) shows pronounced modulations as illustrated in Fig. 4.

The electron density surrounding the point charge $Z_1 e$ is modulated relative to the mean density n by

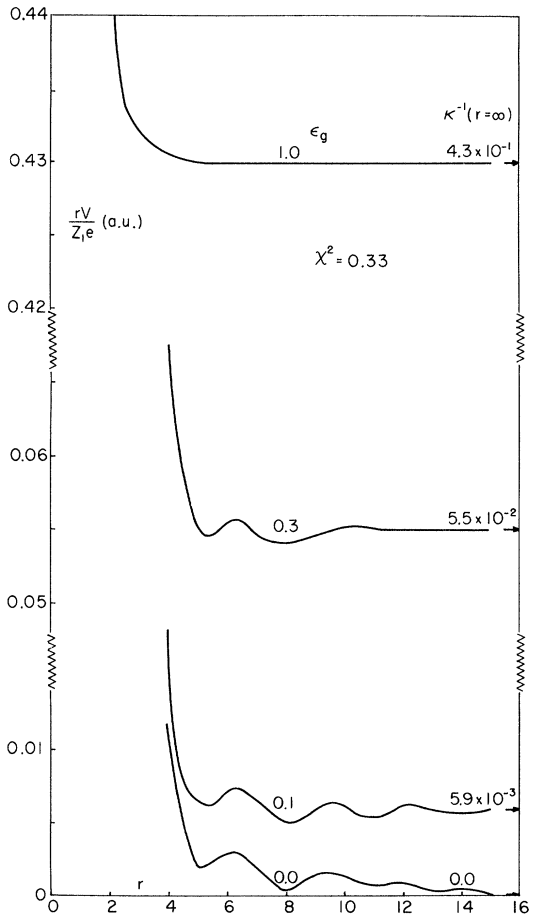

FIG. 4. Screening function of the potential of a fixed positive point charge in a semiconductor $r_s = 2$. For $r \to 0$ the curves rise to the value 1. The asymptotic values for large r, $\kappa^{-1}(0, 0, E_g)$, are indicated by the arrows.

$$\frac{\Delta n}{Z_1 e n} = \frac{1}{2\pi^2 r^2}\int_0^\infty x\, dx \sin x\left[1 - \kappa^{-1}\left(\frac{\pi\chi^2 x}{2r}, 0, E_g\right)\right], \quad (15)$$

as illustrated in Fig. 5. In the limit $E_g \to 0$ the modulations reduce to the well-known periodic Friedel oscillations of the electron gas $\sim (\cos 2k_F r)/(2k_F r)^3$. They are caused by the singularity of $d\kappa(q, 0, 0)/dq$ at $q = 2k_F$. When $E_g > 0$, no such singularity is included in the domain of integration in Eq. (2). As a consequence, the oscillations are damped and their period increases with r.

Noted parenthetically, the disappearance of the singularity in $d\kappa/dq$ with $E_g > 0$ suggests that, by comparison with metals, the Kohn effect[24,25] in solids with band gaps can at best be observed in a damped form.

The annihilation rate of positrons λ is proportional to the electron density at the site $r = 0$ of the annihilating positrons. In the electron gas the polarization by the positron increases the mean density n at $r = 0$ to $n + \Delta n$. Thus

$$\lambda = \lambda_0 \xi = \lambda_0 (1 + \Delta n/n), \quad (16)$$

where $\lambda_0 = 12.0 r_s^{-3}$ nsec^{-1} is the annihilation rate in the absence of polarization. The term in parentheses in Eq. (16) defines the density enhancement factor $\xi(r_s)$. It has been calculated in various approximations.[3,4] Neglecting effects of positron inertia, Eq. (15) permits us to calculate a correction factor for materials with an energy gap, $f(r_s, E_g)$ such that

$$\lambda(r_s, E_g) = \lambda_0(r_s)\{1 + f(r_s, E_g)[\xi(r_s) - 1]\}. \quad (17)$$

The factor $f(r_s, E_g)$ is tabulated in Table II. The enhancement factor in the random-phase approximation (RPA) $\xi_{\mathrm{RPA}}(r_s)$ is well approximated by the expression $\xi_{\mathrm{RPA}}(r_s) = 1 + 1.65 r_s^{3/4}$.[26] In higher approximations,[4] $\xi(r_s) \approx 1 + 0.63 r_s^2$.

In general, the experimental annihilation rates of semiconductors and insulators are known to fall below the values expected from the electron-gas model.[27] We illustrate the use of Eq. (17) and predict the positron annihilation rates in Si and Ge by correcting the $\xi(r_s)$ for the electron gas as given by Carbotte[4] with the appropriate values of $f(r_s, E_g)$. We obtain $\lambda(\mathrm{Si}) = 4.08$ nsec^{-1} and $\lambda(\mathrm{Ge}) = 4.55$ nsec^{-1}. The most recent experimental values are $\lambda(\mathrm{Si}) = (4.00 \pm 0.08)$ nsec^{-1}, and $\lambda(\mathrm{Ge}) = (4.24 \pm 0.12)$ nsec^{-1}.[28]

IV. STOPPING POWER FOR HEAVY CHARGED PARTICLES

The electronic stopping power of a dispersive medium for a particle of charge $Z_1 e$ and velocity v_1 is given by

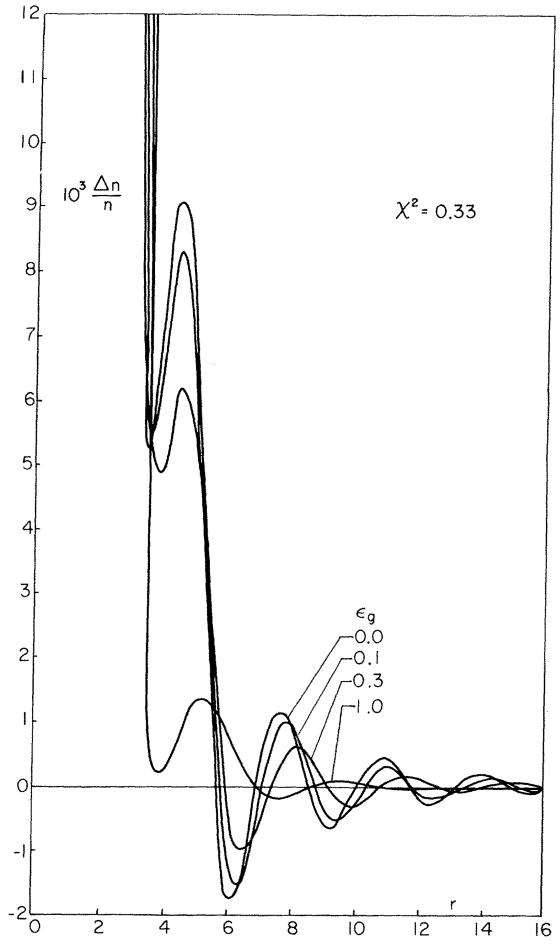

FIG. 5. Displaced density around a fixed positive point charge in a semiconductor $r_s = 2$.

$$-\frac{dE}{dx} = \frac{Z_1^2 e^2 \omega_p^2}{v_1^2} L , \tag{18}$$

where L is the stopping number per target electron

$$L = \frac{6}{\pi \chi^2} \int_0^{v/v_F} u\, du \int_0^\infty z\, dz \mathrm{Im}[\kappa^{-1}(z, u, E_g) - 1]. \tag{19}$$

One can distinguish two types of contributions to L,

$$L = L_s + L_r . \tag{20}$$

The first, L_s, comes from close single collisions. It is equal to the double integral in Eq. (19) under conditions such that $\mathrm{Im}\kappa \neq 0$. The second L_r comes from collective resonance excitations of the system. It corresponds to conditions where $\mathrm{Im}\kappa = 0$ and the real part, through $\mathrm{Re}\kappa = 0$, satisfies a dispersion relation. The contribution from collective excitations is given by the line integral

$$L_r = \int_0^\infty \frac{dz}{z} \left[6uz \left(\frac{\partial \kappa(z, u, E_g)}{\partial u} \right)^{-1} \right]_{\kappa = 0} . \tag{21}$$

The properties of L have been studied for the electron gas ($E_g = 0$).[5] The importance of collective excitations for the stopping power of insulators has been pointed out previously.[17]

The properties of the integrand in Eqs. (19) and (21) for the model semiconductors are discussed elsewhere.[23] The most conspicuous feature for finite E_g is a contribution from umklapp processes to the losses in close collisions in the long-wavelength domain. In the limit of high particle velocities, we make use of the long-wavelength limit of the response function and obtain

$$L(v_1, E_g) = \ln y(v_1, E_g), \tag{22}$$

where

$$y = 2v_1^2/(\omega_p^2 + E_g^2)^{1/2} \tag{23}$$

is a reduced variable proportional to the particle energy. In the limit $E_g \to 0$ we obtain the stopping-power formula for an electron gas.

It is of particular interest to study the relative magnitude of L_s and L_r. The contribution L_r from collective oscillations sets in at particle velocities such that $y > y_c$. The constant y_c is a measure of the threshold energy for the onset of undamped collective oscillations. It is defined by the intersection of the curves $\kappa_1(z, u, E_g) = 0$ and $\kappa_2(z, u, E_g) = 0$, and shown in Fig. 6. The range of particle velocities in which collective excitations do not contribute to the stopping power grows with E_g. The stopping function at $y = y_c = 2v_{1c}^2/(\omega_p^2 + E_g^2)^{1/2}$ is a characteristic constant $L = L_s = C(y_c, E_g)$ plotted in Fig. 7.

Bohr found that the energy lost by swift charged particles to atoms in close collisions should be nearly equal to the energy lost in distance collisions.[29] This "equipartition" was examined by Lindhard and Winther.[5] They proved that a parti-

TABLE II. Enhancement correction factor $f(r_s, \epsilon_g)$. For the electron gas, $f(r_s, \epsilon_g = 0) = 1.00$.

χ^2	r_s	$f(r_s, \epsilon_g)$ $\epsilon_g = 0.2$	0.4	0.6	0.8	1.0
0.1	0.6	0.941	0.866	0.785	0.705	0.632
0.2	1.2	0.951	0.885	0.820	0.749	0.683
0.3	1.8	0.956	0.901	0.829	0.778	0.714
0.4	2.4	0.959	0.908	0.851	0.794	0.737
0.5	3.0	0.960	0.915	0.864	0.808	0.755
0.6	3.6	0.963	0.921	0.872	0.821	0.770
0.7	4.2	0.965	0.923	0.880	0.830	0.781
0.8	4.8	0.966	0.929	0.886	0.841	0.792
0.9	5.4	0.967	0.931	0.890	0.847	0.801
1.0	6.0	0.968	0.933	0.895	0.852	0.808

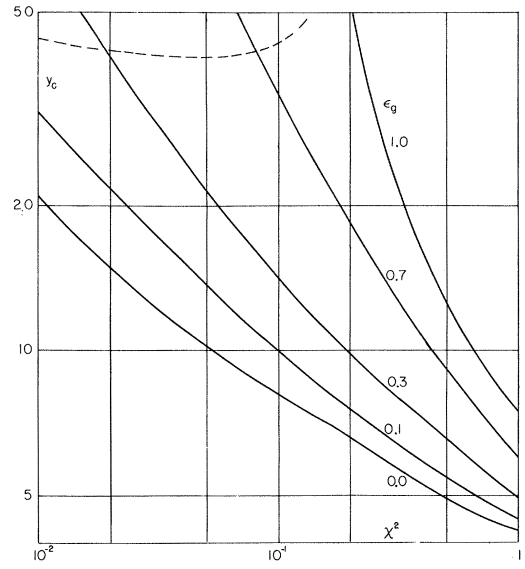

FIG. 6. Collective excitations contribute to the stopping power of the valence electrons in a semiconductor when $y > y_c(\chi^2, E_g)$, Eq. (23). The approximations are valid below the dashed line corresponding to $E_g/\omega_p = 1$.

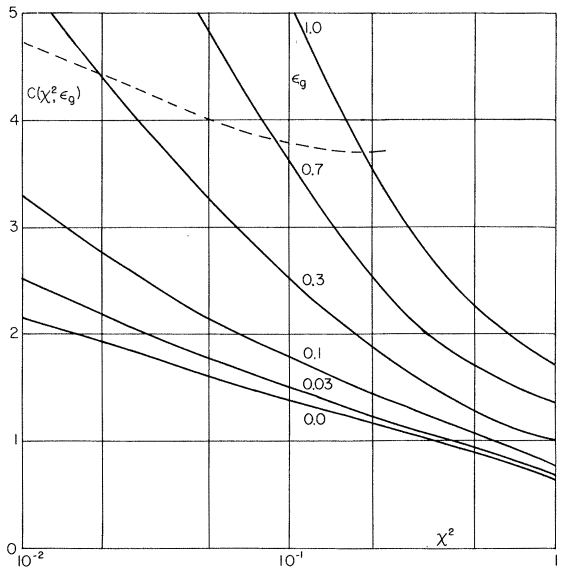

FIG. 7. Constant $C(\chi^2, E_g)$ in the partition rule (25) for the valence electrons in semiconductors. The approximations are valid below the dashed line corresponding to $E_g/\omega_p = 1$.

tion rule holds for the uniform electron gas. We have investigated the partition for the electron gas with an energy gap, and find that the equipartition rule

$$\frac{dL_r(v_1, \chi^2, E_g)}{dv_1} = \frac{dL_s(v_1, \chi^2, E_g)}{dv_1}, \quad v > v_c \tag{24}$$

holds for $E_g \geq 0$. That is,

$$L_s(y, E_g) = C(y_c, E_g) + L_r(y, E_g), \quad y \geq y_c. \tag{25}$$

The constant $C(y_c, E_g)$ gives a quantitative measure for the result that, as E_g increases, relatively more single-particle excitations than collective excitations contribute to the energy loss in the valence electron gas of a semiconductor. Examples are given in Table III and Fig. 8. L_s and L_r become asymptotically equal only at particle velocities so high that $[C(y, E_g)/\ln y] \ll 1$.

The shift of the energy loss from collective excitations to single-particle excitations with increasing E_g comes mathematically from the branch of the integrand of Eq. (19) displayed earlier which has a negative slope in the u, z plane just as the plasma resonance curve.[23] It is caused by umklapp processes in the long-wavelength domain. The proof of the partition rule is a simple extension of the proof for the electron gas, because this branch corresponds to zeros of κ in the complex z^2 plane that place single-particle poles for κ^{-1} along with the plasma pole below the real axis. In performing the integration, Eq. (19), the contour

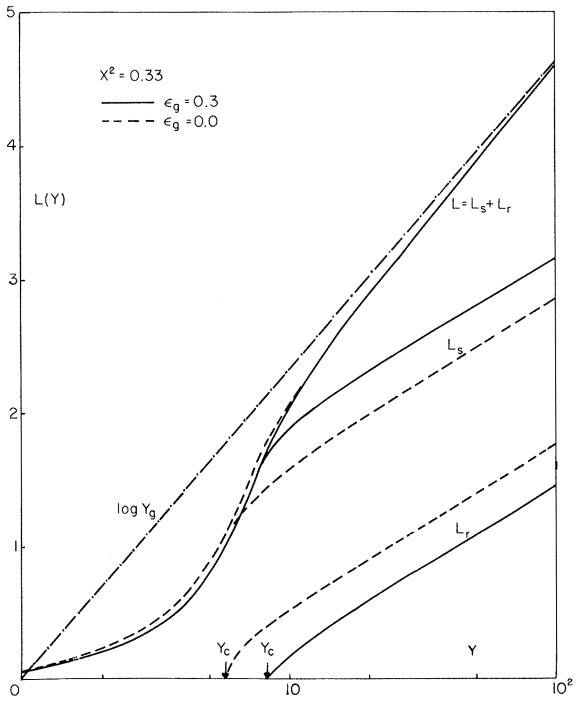

FIG. 8. Contributions from close single collisions L_s and from distant resonance collisions L_r add up to a stopping function L that is insensitive to changes in E_g if scaled in terms of y, Eq. (23).

TABLE III. Stopping functions L_s and L_r as a function of y. The total stopping function $L = L_s + L_r$. Asymptotically for large y, $L = \ln y$.. The notation $R(x)$ means $R \times 10^x$.

χ^2			0.1			
r_s			0.6			
ϵ_g	0		0.1		0.32	
y	L_s	L_r	L_s	L_r	L_s	L_r
1.000 (−1)	1.942 (−3)		1.742 (−3)		8.424 (−4)	
1.585 (−1)	3.875 (−3)		3.557 (−3)		2.271 (−3)	
2.512 (−1)	7.730 (−3)		7.202 (−3)		5.442 (−3)	
3.981 (−1)	1.542 (−2)		1.451 (−2)		1.215 (−2)	
6.310 (−1)	3.073 (−2)		2.910 (−2)		2.607 (−2)	
1.000 (0)	6.118 (−2)		5.824 (−2)		5.442 (−2)	
1.585 (0)	1.216 (−1)		1.162 (−1)		1.116 (−1)	
2.512 (0)	2.409 (−1)		2.310 (−1)		2.260 (−1)	
3.981 (0)	4.750 (−1)		4.561 (−1)		4.517 (−1)	
6.310 (0)	9.316 (−1)		8.927 (−1)		8.887 (−1)	
1.000 (1)	1.623 (0)	2.138 (−1)	1.756 (0)		1.700 (0)	
1.585 (1)	1.963 (0)	5.536 (−1)	2.141 (0)	3.729 (−1)	2.518 (0)	4.000 (−3)
2.512 (1)	2.243 (0)	8.342 (−1)	2.423 (0)	6.542 (−1)	2.798 (0)	2.784 (−1)
3.981 (1)	2.502 (0)	1.093 (0)	2.682 (0)	9.130 (−1)	3.059 (0)	5.365 (−1)
6.310 (1)	2.749 (0)	1.340 (0)	2.928 (0)	1.159 (0)	3.306 (0)	7.835 (−1)
1.000 (2)	2.990 (0)	1.581 (0)	3.169 (0)	1.400 (0)	3.547 (0)	1.025 (0)
1.585 (2)	3.226 (0)	1.817 (0)	3.406 (0)	1.637 (0)	3.783 (0)	1.261 (0)
2.512 (2)	3.460 (0)	2.052 (0)	3.641 (0)	1.872 (0)	4.017 (0)	1.495 (0)
3.981 (2)	3.693 (0)	2.284 (0)	3.873 (0)	2.105 (0)	4.250 (0)	1.728 (0)
6.310 (2)	3.923 (0)	2.514 (0)	4.103 (0)	2.334 (0)	4.479 (0)	1.958 (0)
1.000 (3)	4.155 (0)	2.746 (0)	4.335 (0)	2.566 (0)	4.711 (0)	2.190 (0)
$\left(\frac{v_1}{v_F}\right)^2 \Big/ y$	0.182		0.184		0.199	
y_c	8.29		10.05		14.06	
$C(y_c, E_g)$	1.410		1.769		2.522	
E_g(eV)	0		13.9		43	

χ^2			0.33			
r_s			2.0			
ϵ_g	0		0.1		0.32	
y	L_s	L_r	L_s	L_r	L_s	L_r
1.000(−1)	2.285 (−3)		2.109 (−3)		1.501 (−3)	
1.585(−1)	4.576 (−3)		4.257 (−3)		3.374 (−3)	
2.512(−1)	9.173 (−3)		8.593 (−3)		7.247 (−3)	
3.981(−1)	1.841 (−2)		1.734 (−2)		1.521 (−2)	
6.310(−1)	3.701 (−2)		3.505 (−2)		3.155 (−2)	
1.000 (0)	7.451 (−2)		7.089 (−2)		6.510 (−2)	
1.585 (0)	1.503 (−1)		1.436 (−1)		1.339 (−1)	
2.512 (0)	3.037 (−1)		2.912 (−1)		2.748 (−1)	
3.981 (0)	6.169 (−1)		5.922 (−1)		5.629 (−1)	
6.310 (0)	1.234 (0)	1.468 (−1)	1.241 (0)		1.154 (0)	
1.000 (1)	1.581 (0)	4.932 (−1)	1.674 (0)	3.774 (−1)	1.896 (0)	1.763 (−1)
1.585 (1)	1.860 (0)	7.721 (−1)	1.962 (0)	6.652 (−1)	2.175 (0)	4.569 (−1)
2.512 (1)	2.116 (0)	1.029 (0)	2.222 (0)	9.237 (−1)	2.432 (0)	7.143 (−1)
3.981 (1)	2.362 (0)	1.274 (0)	2.467 (0)	1.169 (0)	2.677 (0)	9.592 (−1)
6.310 (1)	2.601 (0)	1.514 (0)	2.706 (0)	1.409 (0)	2.917 (0)	1.199 (0)
1.000 (2)	2.837 (0)	1.749 (0)	2.942 (0)	1.645 (0)	3.152 (0)	1.434 (0)
1.585 (2)	3.071 (0)	1.983 (0)	3.176 (0)	1.878 (0)	3.386 (0)	1.668 (0)
2.512 (2)	3.303 (0)	2.216 (0)	3.408 (0)	2.111 (0)	3.619 (0)	1.901 (0)
3.981 (2)	3.535 (0)	2.447 (0)	3.640 (0)	2.343 (0)	3.850 (0)	2.132 (0)
6.310 (2)	3.766 (0)	2.678 (0)	3.870 (0)	2.574 (0)	4.081 (0)	2.363 (0)
1.000 (3)	3.997 (0)	2.912 (0)	4.103 (0)	2.806 (0)	4.314 (0)	2.596 (0)
$\left(\frac{v_1}{v_F}\right)^2 \Big/ y$	0.333		0.334		0.342	
y_c	5.68		6.40		8.11	
$C(y_c, E_g)$	1.086		1.297		1.718	
E_g(eV)	0		1.39		4.3	

Table III (*Continued*)

χ^2												
r_s					1.0							
ϵ_g					6.0							
	0				0.1				0.32			
y	L_s		L_r		L_s		L_r		L_s		L_r	
1.000(−1)	1.967 (−3)				1.816 (−3)				1.468 (−3)			
1.585(−1)	4.009 (−3)				3.728 (−3)				3.133 (−3)			
2.512(−1)	8.222 (−3)				7.697 (−3)				6.653 (−3)			
3.981(−1)	1.698 (−2)				1.601 (−2)				1.415 (−2)			
6.310(−1)	3.537 (−2)				3.355 (−2)				3.022 (−2)			
1.000 (0)	7.432 (−2)				7.096 (−2)				6.498 (−2)			
1.585 (0)	1.578 (−1)				1.515 (−1)				1.407 (−1)			
2.512 (0)	3.394 (−1)				3.272 (−1)				3.071 (−1)			
3.981 (0)	7.550 (−1)				7.247 (−1)				6.816 (−1)			
6.310 (0)	1.205	(0)	4.063 (−1)		1.226	(0)	3.350 (−1)		1.275	(0)	2.548 (−1)	
1.000 (1)	1.488	(0)	6.895 (−1)		1.534	(0)	6.432 (−1)		1.584	(0)	5.635 (−1)	
1.585 (1)	1.744	(0)	9.458 (−1)		1.790	(0)	8.995 (−1)		1.855	(0)	8.346 (−1)	
2.512 (1)	1.989	(0)	1.190	(0)	2.035	(0)	1.144	(0)	2.100	(0)	1.079	(0)
3.981 (1)	2.228	(0)	1.429	(0)	2.274	(0)	1.383	(0)	2.336	(0)	1.318	(0)
6.310 (1)	2.463	(0)	1.665	(0)	2.510	(0)	1.619	(0)	2.575	(0)	1.554	(0)
1.000 (2)	2.696	(0)	1.898	(0)	2.743	(0)	1.852	(0)	2.808	(0)	1.787	(0)
1.585 (2)	2.929	(0)	2.130	(0)	2.975	(0)	2.084	(0)	3.040	(0)	2.019	(0)
2.512 (2)	3.160	(0)	2.362	(0)	3.207	(0)	2.316	(0)	3.272	(0)	2.251	(0)
3.981 (2)	3.391	(0)	2.593	(0)	3.438	(0)	2.547	(0)	3.503	(0)	2.482	(0)
6.310 (2)	3.622	(0)	2.823	(0)	3.668	(0)	2.777	(0)	3.733	(0)	2.712	(0)
1.000 (3)	3.853	(0)	3.052	(0)	3.898	(0)	3.007	(0)	3.963	(0)	2.942	(0)
$\left(\frac{v_1}{v_F}\right)^2 \Big/ y$	0.575				0.518				0.582			
y_c	4.15				4.42				4.93			
$C(y_c, E_g)$	0.799				0.891				1.021			
E_g(eV)	0				0.14				0.43			

χ^2								
r_s								
ϵ_g								
	1.0							
y	L_s		L_r		L_s		L_r	
1.000(−1)					1.479 (−10)			
1.585(−1)					4.856 (−4)			
2.512(−1)					2.568 (−3)			
3.981(−1)					7.762 (−3)			
6.310(−1)					2.016 (−2)			
1.000 (0)					4.913 (−2)			
1.585 (0)					1.160 (−1)			
2.512 (0)					2.685 (−1)			
3.981 (0)					6.139 (−1)			
6.310 (0)	1.275	(0)	2.548 (−1)		1.419	(0)		
1.000 (1)	1.584	(0)	5.635 (−1)		1.882	(0)	2.960 (−1)	
1.585 (1)	1.855	(0)	8.346 (−1)		2.138	(0)	5.520 (−1)	
2.512 (1)	2.100	(0)	1.079	(0)	2.383	(0)	7.970 (−1)	
3.981 (1)	2.336	(0)	1.318	(0)	2.622	(0)	1.036	(0)
6.310 (1)	2.575	(0)	1.554	(0)	2.857	(0)	1.271	(0)
1.000 (2)	2.808	(0)	1.787	(0)	3.091	(0)	1.505	(0)
1.585 (2)	3.040	(0)	2.019	(0)	3.323	(0)	1.737	(0)
2.512 (2)	3.272	(0)	2.251	(0)	3.554	(0)	1.968	(0)
3.981 (2)	3.503	(0)	2.482	(0)	3.785	(0)	2.199	(0)
6.310 (2)	3.733	(0)	2.712	(0)	4.016	(0)	2.430	(0)
1.000 (3)	3.963	(0)	2.942	(0)	4.245	(0)	2.659	(0)
$\left(\frac{v_1}{v_F}\right)^2 \Big/ y$	0.630							
y_c	7.49							
$C(y_c, E_g)$	1.586							
E_g(eV)	1.39							

circles these poles and the collective resonance pole in the same sense. The relative contribution of collective excitations diminishes as more poles shift below the axis when E_g increases. The equality of the incremental changes of L_s and L_r, Eq. (24), remains unaffected. Although the umklapp processes cause the relative contributions of $L_s(y, E_g)$ and $L_r(y, E_g)$ to vary sharply with E_g, the total stopping function $L(y)$ depends on E_g essentially only through ν.

*Permanent address: Aerospace Corp., San Bernardino, Calif.

[1]J. Langer and S. Vosko, J. Phys. Chem. Solids 12, 196 (1959).

[2]E. Sziklas, Phys. Rev. 138, A1070 (1965).

[3]S. Kahana, Phys. Rev. 129, 1622 (1963).

[4]J. Carbotte, Phys. Rev. 155, 197 (1967), and references cited therein.

[5]J. Lindhard and A. Winther, Kgl. Danske Videnskab. Selskab, Mat.-Fys. Medd. 34, No. 4 (1964).

[6]W. Brandt and S. Lundqvist, Phys. Rev. 139, A612 (1965).

[7]W. Brandt and S. Lundqvist, J. Quant. Spectry. Radiative Transfer 7, 411 (1967).

[8]D. Penn, Phys. Rev. 128, 2093 (1963).

[9]J. Callaway, Phys. Rev. 116, 1368 (1959).

[10]G. Gandel'man and V. Ermachenko, Zh. Eksperim. i Teor. Fiz. 45, 522 (1963) [Soviet Phys. JETP 18, 358 (1964)].

[11]A. Bardasis and D. Hone, Phys. Rev. 153, 849 (1967).

[12]H. Ehrenreich and M. H. Cohen, Phys. Rev. 115, 786 (1959). In the following, atomic units $m = |e| = \hbar = 1$ are used, except when stated otherwise.

[13]J. Fry, Phys. Rev. 179, 892 (1969).

[14]J. Reinheimer, Ph.D. thesis, New York University, 1968 (University Microfilms Inc. No. 61/7988, Ann Arbor, Mich.) (unpublished). Copies of the FORTRAN listing of the computer program for the response function [Eq. (4)] can be obtained from the authors on request.

[15]J. Lindhard, Kgl. Danske Videnskab. Selskab, Mat.-Fys. Medd. 28, No. 4 (1954).

[16]J. Lindhard and M. Scharff, Kgl. Danske Videnskab. Selskab, Mat.-Fys. Medd. 27, No. 15 (1953).

[17]W. Brandt, Phys. Rev. 112, 1624 (1958).

[18]W. Brandt and S. Lundqvist, Arkiv Fysik 28, 399 (1965).

[19]W. Brandt, L. Eder, and S. Lundqvist, J. Quant. Spectry. Radiative Transfer 7, 185 (1967).

[20]H. Nara, J. Phys. Soc. Japan 20, 1097 (1965).

[21]G. Srinivasan, Phys. Rev. 178, 1244 (1969).

[22]In Eq. (11), E_g has been inserted for the formally more correct $E_g(1-\gamma)^{-1/2}$. Penn's static interpolation formula applies to the case $\omega = \gamma_m = 0$ and $s^2 = E_g$, i.e., $\epsilon_g = \frac{2}{3}$.

[23]W. Brandt and J. Reinheimer, Can. J. Phys. 46 607 (1968).

[24]W. Kohn, Phys. Rev. Letters 2 393 (1959).
[25]E. Woll and W. Kohn, Phys. Rev. 126, 1693 (1962).
[26]W. Brandt, L. Eder, and S. Lundqvist, Phys. Rev. 142, 165 (1966).
[27]H. Weisberg and S. Berko, Phys. Rev. 154, 249 (1967).
[28]R. Fieschi, A. Gafnetti, C. Ghezzi, and M. Martial, Phys. Rev. 175, 393 (1968).
[29]N. Bohr, Kgl. Danske Videnskab. Selskab, Mat.-Fys. Medd. 18, No. 8 (1948).

PHYSICAL REVIEW B VOLUME 2, NUMBER 8 15 OCTOBER 1970

Electrical and Optical Properties of Narrow-Band Materials

David Adler
Department of Electrical Engineering and Center for Materials Science and Engineering, Massachusetts Institute of Technology, Cambridge, Massachusetts* 02139
and
Julius Feinleib
Energy Conversion Devices, Inc., 1675 *West Maple Road, Troy, Michigan* 48084
(Received 13 January 1970)

The electrical and optical properties of materials which are characterized by narrow bands in the vicinity of the Fermi energy are discussed. For such materials, electronic correlations and the electron-phonon coupling must be considered explicitly. Correlations in f bands and in extremely narrow d bands can be handled in the ionic limit of the Hubbard Hamiltonian. It is shown that free carriers in such bands form small polarons which contribute to conduction only by means of thermally activated hopping. Wider bands may also exist near the Fermi energy. Carriers in these bands may form large polarons and give a bandlike contribution to conductivity. A model is proposed for determining the density of states of pure stoichiometric crystals, beginning with the free-ion energy levels, and taking into account the Madelung potential, screening and covalency effects, crystalline-field stabilizations, and overlap effects. Exciton states are considered explicitly. The Franck-Condon principle necessitates the construction of different densities of states for electrical conductivity and optical absorption. Because of the bulk of experimental data presently available, the model is applied primarily to NiO. The many-particle density of states of pure stoichiometric NiO is calculated and is shown to be in agreement with the available experimental data. When impurities are present or nonstoichiometry exists, additional transitions must be discussed from first principles. The case of Li-doped NiO is discussed in detail. The calculations are consistent with the large mass of experimental information on this material. It is concluded that the predominant mechanism for conduction between 200 and 1000 °K is the transport of hole-like large polarons in the oxygen $2p$ band. A method for representing the many-particle density of states on an effective one-electron diagram is discussed. It is shown that if correlations are important, donor or acceptor levels cannot be drawn as localized levels in the energy gap when multiple conduction or valence bands are present. This result comes about because extrinsic ionization energies of two correlated bands differ by an energy which bears no simple relation to the difference in energies of the intrinsic excitations, which are conventionally used to determine the relative positions of the bands.

I. INTRODUCTION

Transition-metal and rare-earth compounds are characterized by d and f bands in the vicinity of the Fermi energy. Since the spatial extent of these electrons away from their ion cores is relatively small compared to outer s and p electrons, the d and f states on nearest-neighboring ions overlap only slightly and thus ordinarily form very narrow bands. It might be asked whether there is any meaning in referring to these somewhat spread out levels as bands rather than localized states, since they are certainly not one-electron bands in the ordinary sense. However, long-range magnetic order is the rule rather than the exception in these materials, and so the effective overlap must be finite.

These materials can be either insulating or metallic.[1] However, for a large class, e.g., CoO, band theory appears to fail. In these compounds, it can be shown by symmetry arguments that a partially filled band must exist, and yet they are excellent insulators. Although attempts at modifying band theory to explain the insulating behavior have been made,[2] and these have succeeded in reducing the number of materials in the class,[3] it does not appear likely that a pure Hartree-Fock approach